The isotopic composition of Cadmium in the water column of the South China Sea

Shun-Chung Yang [a,b,c], Der-Chuen Lee [a,*], Tung-Yuan Ho [b]

[a] *Institute of Earth Sciences, Academia Sinica, Taipei, Taiwan*
[b] *Research Center for Environmental Changes, Academia Sinica, Taipei, Taiwan*
[c] *Department of Geosciences, National Taiwan University, Taipei, Taiwan*

Abstract

We determined the Cd isotopic composition of seawater and sinking particles collected in the deep basin of the northern South China Sea (SCS) to investigate the controlling mechanisms on the Cd isotopic composition in the water column. The isotopic composition in the water column decreased with depth, with $\varepsilon^{114/110}Cd$ values ($\varepsilon^{114/110}Cd = [(^{114}Cd/^{110}Cd)_{sample}/(^{114}Cd/^{110}Cd)_{JMC\ Cd\ Münster} - 1] \times 10^4$) ranging from +8.7 to +9.9 in the top 80 m, from +4.6 to +5.5 between 100 and 150 m, decreasing from +5.5 to +3.6 at depths from 150 to 1000 m, and remaining at $+3.4 \pm 0.5$ from 1000 to 3500 m. The isotopic composition and concentrations of Cd observed in the deep waters of the SCS are similar to the values that were previously reported in the North Pacific Ocean. In the thermocline, the variations in the Cd isotopic composition and concentrations were consistent with the relative volumetric percentages of the subsurface water, the intermediate water, and the deep water in the water column, indicating that water mixing is the dominant process determining the isotopic composition in the thermocline. Comparable to the isotopic composition value in the seawater of the mixed layer, the $\varepsilon^{114/110}Cd$ in the sinking particles collected at 30 m was $+9.3 \pm 0.9$. Because our previous studies demonstrated that the particulate Cd was predominantly biogenic organic matter, the comparable isotopic composition between the surface seawater and the sinking particles indicates that net biological isotopic fractionation on Cd in the surface water was insignificant. The result indicates that phytoplankton do not necessarily take up relatively light Cd in the oceanic surface waters. It is necessary to directly and systematically investigate how marine phytoplankton fractionate Cd isotopes.

1. INTRODUCTION

Cadmium is biologically cycled in the marine water column, taken up by phytoplankton in the surface waters and subsequently regenerated and recycled in the water column. The vertical distribution pattern of Cd is identical to those of major nutrients in the oceans (Boyle et al., 1976; Bruland, 1980). Horizontally, the Cd/P ratios in global deep waters are relatively consistent among various oceans, without significant changes with the age of seawater. In addition, Cd/P ratios in the water column are fairly close to the averaged ratio in phytoplankton assemblages, which has been obtained through both field and laboratory culture studies (Ho et al., 2003; Ho, 2006). The comparable results between various field and laboratory culture studies indicate that particulate Cd in the ocean is largely intracellular (Ho, 2006). Based on these close, linear correlations, Cd concentrations have been considered an analog of phosphate concentrations in ancient seawater (Boyle, 1988). Consequently, Cd/Ca ratios in foraminiferal fossil shells have been proposed as a proxy to evaluate phosphate concentrations in the paleo-oceans (Boyle, 1988; Elderfield and Rickaby, 2000).

Compared to other essential trace metals, the cycling of Cd exhibits several unique features. Particulate Cd in the

---

* Corresponding author. Address: 128, Sec. 2, Academia Rd, Nankang, Taipei 115, Taiwan. Tel.: +886 2 27839910x617.
  E-mail address: dclee@earth.sinica.edu.tw (D.-C. Lee).

ocean is primarily biogenic because Cd concentrations are relatively high in biogenic particles and extremely low in lithogenic particles. In terms of the ratios to major elements in lithogenic and biogenic particles, Cd is equivalent to 0.0006 mmol/mol Al in lithogenic particles but is up to 0.2 mmol/mol P in biogenic particles (Ho et al., 2009), which indicates that Cd concentrations in biogenic particles are 20-fold higher than those of lithogenic particles with the same weight. Thus, vertical transport of particulate Cd primarily occurs via biogenic particles in the open ocean, where biogenic particles are the dominant material in sinking particles. In addition, Cd removal rates in most oceanic surface water are extremely efficient due to the low Cd input and high biological uptake of Cd. Recent studies in the SCS have observed that many trace metals except Cd are largely adsorbed on phytoplankton cellular surfaces and sinking particles in the surface water due to the high aeolian input of anthropogenic aerosols in the region (Ho et al., 2007, 2010). The Cd determined in the sinking particles was mainly intracellular (Ho et al., 2009, 2010). Most importantly, unlike particle-reactive trace metals, dissolved Cd in oceanic deep water, which originates from the decomposition of biogenic particles, is not subject to scavenging and may thereby preserve the signals of the biogeochemical processes in oceanic surface water. Thus, Cd isotopic composition in the marine water column or environmental recorders may be a potential proxy to decipher these signals.

The processes controlling Cd cycling and input in marine water columns, including atmospheric inputs, biological uptake and cycling, the vertical transport of particles, and water mass exchange and upwelling, should be studied to fully understand their relative importance on Cd cycling. However, Cd concentrations alone provide limited information to study these processes because Cd concentrations exhibit comparable vertical and lateral patterns in the ocean, with nutrient-type profiles in most oceanic regions. Isotopic composition of Cd in the seawater may shed light to enable further understanding of these controlling processes. The study of Cd isotopic composition in the ocean is still at its beginning stages. Ripperger et al. (2007) observed that the majority of their global seawater samples exhibited an inverse relationship between dissolved Cd concentrations and $\varepsilon^{114/110}$Cd, ranging from $+3 \pm 0.5$ for most oceanic deep waters to $+38 \pm 6$ in an oceanic surface water sample with extremely low Cd concentration. The authors suggested that the Cd isotopic variations reflect the preferential uptake of light isotopes by phytoplankton in a closed-system Rayleigh distillation model. However, the assumption of the fractionation effect by marine phytoplankton is simply based on results observed by freshwater microalgae culture experiments (Lacan et al., 2006) and systemic study on marine phytoplankton uptake on Cd isotopic fractionation is still lacking. Furthermore, Abouchami et al. (2011) studied the marine biological fractionation by determining Cd isotopes in the surface waters of the Southern Ocean and suggested that the magnitude of fractionation in surface water can also be related to phytoplankton community structure.

Although Ripperger et al. (2007) has revealed a consistent Cd isotopic composition in oceanic deep waters, the Cd isotopic composition in oceanic surface waters and thermocline are still limited. The mechanisms controlling the isotopic composition variations in the marine water column are not fully understood. Taking the advantage of the previous studies in the SCS, which have reported the sources and sinks of Cd (Ho et al., 2009, 2010), and the physical movement of the water masses in the studied site (Chen et al., 2001; Qu et al., 2006; Liu et al., 2010), we determined the Cd isotopic composition of seawater and sinking particles in an offshore water column of the SCS to investigate how the elemental and isotopic compositions are controlled in the water column, particularly focusing on the surface water layer and the thermocline.

2. MATERIALS AND METHODS

2.1. Sampling site

Seawater samples and sinking particles were collected at the northern SCS deep water time series station known as the South East Asian Time Series (SEATS). The SEATS station is located at 18′16.358°N, 115′41.178°E with a bottom depth of 3783 m (Fig. 1). The semi-closed SCS is the largest marginal sea in the world. The water of the northern SCS primarily exchanges with the water in the Western Philippine Sea through the Luzon Strait (Fig. 1). Detailed information regarding water mass exchange may be found in the studies of Qu et al. (2000, 2006) and Liu et al. (2010). Background on the biogeochemical characteristics of the SCS can be found in a study by Wong et al. (2007). Attributed to the larger population in the developing countries surrounding the SCS, the input of anthropogenic aerosols from the burning of fossil fuels and biomass in the region is significant (Lin et al., 2007). Trace metal inputs to the surface water of the northern SCS also originate from the aeolian deposition of anthropogenic aerosols (Ho et al., 2010).

Detailed information regarding the sampling is described by Ho et al. (2010). In brief, all of the seawater samples were collected with pre acid-cleaned Teflon-coated Go-Flo samplers (General Oceanics) on October 21, 2006 at the SEATS station. The seawater was filtered *in situ* through in-line 0.22 μm acid-cleaned POLYCAP cartridge filters (Whatman) and subsequently transferred to acid-washed polyethylene bottles and were acidified to pH 1 with ultrapure HCl (Seastar). Triplicate seawater samples were collected at each water depth. The sinking particles were collected on a custom-made floating sediment-trap array, which was deployed at the SEATS site at the depths of 30 m for 36 h from October 20 to 22 in 2006. The sinking particle samples were filtered in the land based laboratory through 0.45 μm polycarbonate filters, which were subsequently freeze-dried for further chemical processing and analysis. Although the pore sizes of the filters used for the seawater and sinking particle samples were slightly different, the Cd fraction between 0.22 and 0.45 μm is negligible. Previous study observed that the dissolved Cd concentrations smaller than 0.4 μm were analytically the same as the concentrations smaller than 1 kDa in the seawater of the studied site (Wen et al., 2006). Thus, and the isotopic
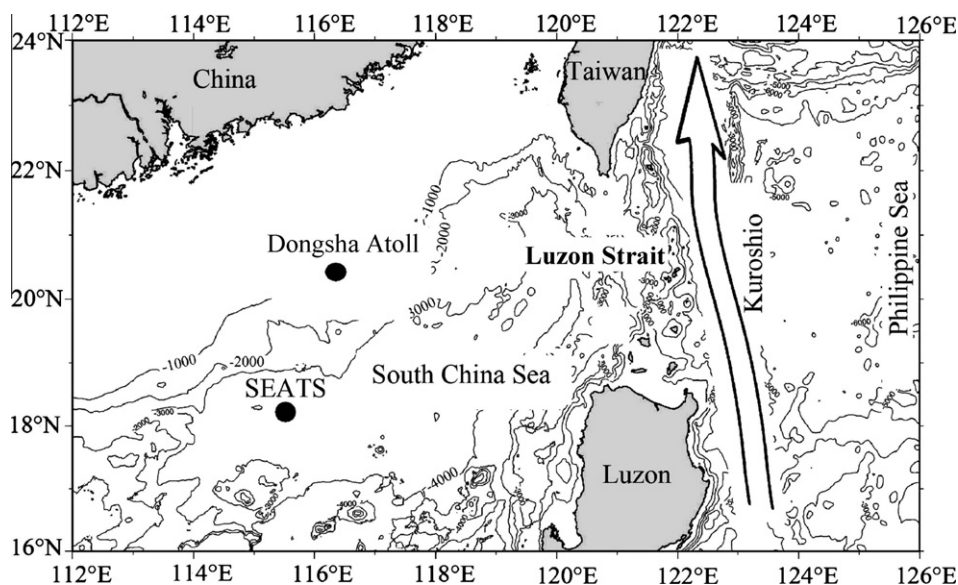
Fig. 1. Location of the sampling sites in the South China Sea. The samples of seawater and sinking particles were collected at SEATS site.

composition in the fraction less than 0.22 μm is representative for dissolved fraction.

2.2. Pretreatment and column chemistry

The double spike technique used in this study was modified from the method of Ripperger and Rehkamper (2007). Approximately one liter of seawater was used for isotopic composition analysis. Seawater samples were treated with a ^{110}Cd–^{111}Cd double spike containing 171.42 ppb Cd with a ^{111}Cd/^{110}Cd of 0.58847 to achieve a spike to sample ratio of approximately 4. The spiked seawater samples were subsequently acidified to achieve a final HCl concentration of 0.7 N. All of the spiked seawater samples were incubated for at least 3 days to reach a full sample-spike equilibration before the performance of chemical separation procedures.

The sinking particle samples and their blank filters were soaked in a mixture of 1.8 mL of super-pure nitric acid and 0.2 mL of super-pure hydrofluoric acid in 10 mL clean Teflon vials and were subsequently digested in a microwave oven (MARS, CEM) at 180 °C for 15 min with a 10-min ramp from room temperature to 180 °C. After complete digestion, the samples were evaporated to near dryness on the hot plate at 80 °C under a trace-metal clean hood. The particle samples were also spiked with a ^{110}Cd–^{111}Cd double spike, following the same procedures as those used for the seawater samples. The spiked samples were evaporated to dryness on hot plates at 120 °C and subsequently re-dissolved with 0.2 mL super-pure hydrochloric acid. The samples were evaporated to dryness again and were re-dissolved with 1.4 mL of 0.7 N HCl for further column chemistry treatment.

A three-stage column chemistry that was adapted from the study of Ripperger and Rehkamper (2007) was used. Anion resin AG1X8 (Biorad) was applied in the first and the second stages to preconcentrate Cd in the samples and remove major elements, e.g., Na, Mg, and Ca. Another

anion resin, TRU (Eichrom), was applied in the third stage to further remove Mo and Sn to avoid isobaric interference with Cd. The purified Cd samples were evaporated to dryness, and 0.2 mL of super-pure nitric acid was added. The samples were evaporated to dryness again and were re-dissolved with 2% HNO$_3$ to achieve a final sample concentration of approximately 5 ppb Cd. The recovery of Cd was greater than 90%. Any Cd contamination from the sampling and the column chemistry procedures was negligible. The column chemistry blank was at 57 ± 15 picogram (pg) (1SD, $n = 3$), which is equivalent to 1.5% of the Cd in the purified surface water and sinking particle samples and equivalent to 0.1% of the Cd in the purified deep water samples. The filter blank for sinking particles was approximately 23 pg ($n = 3$), which is equivalent to 0.5% of the Cd in the samples.

This method requires only 2.5–5.0 nanogram (ng) of unspiked Cd to reach analytical precision ranging from ± 0.7 to ± 2.9 ε$^{114/110}$Cd (2SD; Table 1). Some other methods may provide slightly better analytical precision but require much larger sample sizes, e.g., the TIMS method requires hundreds of ng of unspiked Cd for each analysis. Similarly, although the method developed by Xue et al. (2011) obtained the precision down to ± 0.5 ε$^{114/110}$Cd (2SD), the natural Cd mass per analysis required 20–30 ng to reach the precision.

2.3. Mass spectrometry analysis

All of the Cd isotopic measurements were performed using a multi-collector ICPMS (Nu Instruments) with a desolvator nebulizer as a sample introduction system (CE-TAC Aridus I) at the Institute of Earth Sciences, Academic Sinica. Four Cd isotopes, 110, 111, 112, and 114, were simultaneously measured in each analysis, and potential isobaric interferences from ^{112}Sn and ^{114}Sn were corrected within-run by simultaneously monitoring ^{118}Sn. Further-

Table 1
The Cd concentrations and isotope composition.

Sample	Depth (m)	Cd (nM)	2SD	$\varepsilon^{114/110}Cd_{JMC}$	$\varepsilon^{114/110}Cd_{NIST}$[a]	2SD	n[c]	2SE[d]
Seawater	20	0.048	0.000	9.0	8.4	2.9	2	2.1
	20[e]	0.048	0.000	10.8	10.2	0.5	2	0.4
	Average	0.048	0.000	9.9	9.3	2.7	4	1.4
	40	0.037	0.000	9.2	8.6	1.4[b]	1	1.4
	40[e]	0.037	0.000	10.1	9.5	1.4[b]	1	1.4
	Average	0.037	0.000	9.6	9.0	0.8	2	0.6
	60	0.041	0.000	9.0	8.4	0.8[b]	1	0.8
	80	0.068	0.000	7.7	7.1	1.4[b]	1	1.4
	80[e]	0.069	0.000	9.2	8.6	0.2	2	0.2
	Average	0.068	0.000	8.7	8.1	1.7	3	1.0
	100	0.242	0.000	4.6	4.0	1.3	7	0.5
	150	0.238	0.000	5.5	4.9	1.3	6	0.5
	300	0.447	0.000	5.4	4.8	1.2	6	0.5
	400	0.541	0.000	5.2	4.6	1.7	9	0.6
	400[e]	0.541	0.000	4.8	4.2	1.1	3	0.7
	Average	0.541	0.001	5.1	4.5	1.6	12	0.4
	500	0.619	0.000	4.9	4.3	1.5	9	0.5
	600	0.648	0.000	4.6	4.0	1.7	12	0.5
	800	0.759	0.000	4.1	3.5	0.9	6	0.4
	800[e]	0.747	0.000	4.4	3.8	1.0	3	0.6
	Average	0.753	0.018	4.2	3.6	0.9	9	0.3
	1000	0.806	0.000	3.6	3.0	1.4	9	0.5
	1500	0.852	0.000	3.3	2.7	1.2	8	0.4
	2000	0.853	0.000	2.7	2.1	2.0	8	0.7
	2000[e]	0.865	0.000	3.9	3.3	1.4	3	0.8
	Average	0.859	0.016	3.0	2.4	2.3	11	0.7
	3000	0.859	0.000	3.6	3.0	1.2	14	0.3
	3500	0.874	0.000	3.4	2.8	1.6	3	0.9
	3500[e]	0.872	0.000	3.5	2.9	0.7	9	0.2
	Average	0.873	0.004	3.5	2.9	1.4	12	0.4
Sinking particles	30	–	–	9.3	8.7	0.9[b]	1	0.9

[a] The $\varepsilon^{114/110}Cd$ values relative to the NIST standard.
[b] Within-day reproducibility (2SD) of Cd IC for Münster JMC standard for the samples with single analysis due to limited Cd mass in the samples.
[c] n: total analysis number.
[d] Uncertainties of the IC data are presented as standard error (2SE), which is calculated by the formula, $2SE = 2SD/n^{0.5}$.
[e] Data of duplicate sampling.

more, ^{105}Pd and $^{64}Zn^{40}Ar$ were monitored separately prior to each analysis to ensure that ^{110}Pd and $^{70}Zn^{40}Ar$ interferences to be negligible. Each measurement, which consisted of 3 blocks with 20 cycles each, consumed approximately 5 ng of Cd.

All of the Cd isotopic compositions are reported as an ε-notation, which is given by the following equation:

$$\varepsilon^{114/110}Cd = [(^{114}Cd/^{110}Cd)_{sample}/(^{114}Cd/^{110}Cd)_{standard} - 1] \times 10^4$$

where the JMC Cd Münster (ICP standard, lot 502552A) was used as the reference standard (2SD = 1.4, n = 69) and the within-day reproducibility ranged from 0.7 to 1.4 ε (2SD, n = 6–9). The accuracy of our method was certified by measurements of the standard reference material BAM-1012 (prepared from Cd metal by the Joint European Project for Primary Isotopic Measurements), Münster-Cd standard solutions (fractionated Cd standard from the University of Münster), and NIST SRM 3108. Our analysis yielded a mean ε$^{114/110}$Cd of −12.0 ± 1.7 (2SD, n = 15) and +45.7 ± 1.4 (2SD, n = 6) for the first two standards, respectively, which were identical to the values compiled by Abouchami et al. (2012), −12.43 ± 0.43 ε and +45.4 ± 0.53 ε. The NIST SRM 3108 obtained a mean ε$^{114/110}$Cd of +0.60 ± 1.0 (2SD, n = 15), which is also consistent within the uncertainties with the certified value, +0.89 ± 0.42 (Abouchami et al., 2012). Our in-house standards Alfa Aesar Cd (plasma standard solution, lot 200880H) and Alfa Aesar Cd Metal (Puratronic Cd metal, lot J16 L23) are also reported with a mean ε$^{114/110}$Cd of +14.0 ± 1.3 (2SD, n = 13) and +11.9 ± 1.6 (2SD, n = 32), respectively.

2.4. Correction for Sn interferences

Trace amounts of Sn existing in samples can cause significant isobaric interference for the Cd isotopic composition analysis (Ripperger and Rehkamper, 2007). The Cd

isotopic composition in the standard JMC Cd Münster doped with various quantities of Sn was determined to evaluate whether the isobaric interference of ^{112}Sn and ^{114}Sn at mass 112 and 114 can be adequately corrected by simultaneously monitoring ^{118}Sn. Fig. 2a demonstrates that Sn interferences can be satisfactorily corrected when the isobaric contribution is less than 0.3% for ^{112}Sn at mass 112 and 0.2% for ^{114}Sn at mass 114. The ^{112}Sn and ^{114}Sn in the purified samples of this study accounted for 0.003–0.11% at mass 112 and 0.002–0.06% at mass 114, respectively, which is within the satisfactorily correctable level (Fig. 2a).
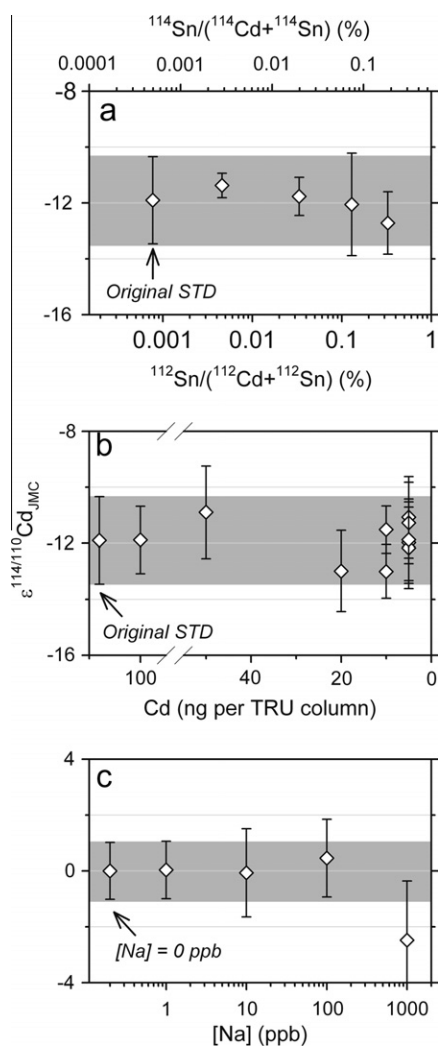

Fig. 2. Evaluation of Sn interference correction, TRU resin matrix, and seawater matrix on Cd IC analysis. The error bars represent standard errors (2SD) of each analysis. (a) The Cd IC of the Alfa Aesar Cd Metal standards doped with various amounts of Sn. (b) The Cd IC of 5–100 ng Cd of Alfa Aesar Cd Metal standards purified by TRU resins. (c) The Cd IC of the JMC Cd Münster standards added with various amounts of trace metal free artificial seawater.

2.5. Evaluation of the matrix effects

The AG1-X8 and TRU resins used in the column chemistry can release organic matter into purified samples (Shiel et al., 2009), which may cause a matrix effect or molecular interferences with the analysis of Cd isotopic composition. The Cd isotopic composition of our in-house Cd standards purified by either AG1-X8 or TRU resins was determined to estimate whether the organic matrix influences the precision and accuracy of isotopic composition measurements. In addition to organic matter, the major ions in seawater, e.g., Na, Mg, and Ca that remain in purified Cd samples may potentially influence the precision and accuracy of the determination of Cd isotopic composition. The Cd isotopic composition of the JMC Cd Münster standard samples, which were added with different trace amounts of trace metal free artificial seawater, were determined to evaluate this effect (Fig. 2c).

Approximately 70 ng of Alfa Aesar Cd was added to 1 l of trace metal clean nature seawater and double-spiked and purified using the first and second column procedures described previously. The eluent for the purified Cd fraction was collected and evaporated to dryness. The dried samples were supplemented with 0.2 mL of super-pure nitric acid and were evaporated to dryness again. The dried samples were re-dissolved with 2% HNO_3 to achieve final total concentrations of approximately 25 ppb. Our analysis yielded a mean $\varepsilon^{114/110}Cd$ of +13.0 ± 0.4 (2SD, $n = 3$) for the purified standard, which is analytically the same as the $\varepsilon^{114/110}Cd$ of +14.0 ± 1.3 in the original standard solution, indicating that the matrix from the AG1-X8 does not significantly influence Cd isotopic measurements.

Previous studies (Shiel et al., 2009; Gault-Ringold and Stirling, 2012) have reported that significant amounts of organic matter are released from TRU resin in column procedures. The organic matter in a purified sample matrix may cause large and anomalous shifts for Cd isotopic composition. The solution of the standard Alfa Aesar Cd metal containing 5–100 ng of Cd was double-spiked and purified by the TRU column procedure to evaluate the influence of the organic matter on Cd isotopic composition analysis. The Cd eluent was processed in the same manner as the matrix effect study for the AG1-X8 resin. Fig. 2b shows that the isotopic composition of the standards with the same amount of Cd but different amounts of TRU matrix solution were statistically similar, demonstrating that the influence of the TRU matrix on the analysis of Cd isotopic composition is also negligible.

Fig. 2c shows that the isotopic composition of the JMC Cd Münster standards, which are enriched with various amounts of trace metal clean natural seawater, purified by Chelex-100 resin (Pai et al., 1990). The results were similar to the value of the original standard when sodium concentrations were within 100 ppb. The isotopic measurements were precise within 1.5 ε (2SD, $n = 3$–6). Because Na concentrations in purified samples were generally less than 1 ppb, this confirms that the remaining major elements in the purified samples did not significantly influence the accuracy and precision of the Cd isotopic analysis.

3. RESULTS AND DISCUSSION

3.1. Cd isotopic composition in the seawater and sinking particles

The Cd concentration and isotopic composition in the water column at the SEATS station are shown in Table 1 and Fig. 3. The vertical variations of the Cd concentrations exhibited a typical nutrient-type profile (Fig. 3a). As for the Cd isotopic composition, the $\varepsilon^{114/110}$Cd ranged between +9 and +10 in the top 80 m and decreased to between +5 to +6 from 100 to 150 m (Fig. 3d). The $\varepsilon^{114/110}$Cd linearly decreased with depth in the thermocline, from +5.5 at 150 m to +3.6 at 1000 m (Fig. 3b). In the deep water, from 1000 to 3500 m, the $\varepsilon^{114/110}$Cd remained constant at approximately $+3.4 \pm 0.5$ (Fig. 3b), which is consistent with the global deep ocean value (Ripperger et al., 2007). The $\varepsilon^{114/110}$Cd in the sinking particles was $+9.3 \pm 0.9$ (2SD), which is similar to the seawater at the top 80 m and is significantly heavier than the seawater from 100 to 3500 m (Fig. 3d).

3.2. A box model for Cd cycling

We established a box model to investigate how particle transport and physical mixing influence Cd cycling in the SCS. The SCS has been intensively studied for physical mixing and particle transports, which include the sources and sinks of Cd in the water column (Ho et al., 2009, 2010, 2011), the vertical mixing of water masses (Qu, 2001; Chen et al., 2001; Wong et al., 2007), and horizontal advection (Qu et al., 2006; Liu et al., 2010). These studies provided a quantitative background to evaluate the relative importance of the processes in the box model. The 3500-m deep water column is separated into 4 boxes based on its biological and physical features. The first layer is the top 100 m zone, where the uptake of phytoplankton on Cd is most active in the water column (Fig. 4a). Based on the T–S plot, there are 3 major water masses in the water column (Figs. 4b and 6a), including the 100–150 m subsurface water mass, the 400–500 m middle layer water mass and the 2000–3500 m deep water mass. Because the three water masses originate from the North Pacific Tropical Water, the North Pacific Intermediate Water, and the West Philippine Sea deep water (Qu et al., 2000, 2006; Liu et al., 2010), we separated the water column below the surface layer into 3 boxes, including 100–250 m subsurface box, the 250–850 m thermocline box, and the 850–3500 m deep water box (Fig. 4b). Based on the concentration data obtained in this study, the averaged Cd concentration in each box is used to calculate the inventory of Cd in each box, which is 0.07, 0.28, 0.62, and 0.85 nM in the boxes from top to bottom, respectively. The primary information concerning the vertical flux and flow rates are shown in Fig. 5a.

3.2.1. The vertical transport of sinking particles

Ho et al. (2009, 2010) has studied and reported the vertical fluxes of Cd at different depths in the water column. Downward Cd fluxes generally follow an exponential decrease with depth. The annually averaged flux was 12 nmol/m²/d at 100 m, decreased to 4.2 nmol/m²/d at 250 m, 1.7 nmol/m²/d at 850 m, and 0.7 nmol/m²/d (Ho et al., 2009, 2010) at 3500 m. The difference between any 2 depths may represent the decomposed vertical Cd fluxes in the box. Because anthropogenic aerosols are known to be the dominant Cd source in surface water (Ho et al., 2010), the decomposed Cd flux in the surface layer may be estimated by the difference between the aerosol deposition fluxes and the sinking particle fluxes at 100 m. A study by Ho et al. (2010) observed that the Cd fluxes at Dongsha Atoll (Fig. 1) in the SCS originated from aerosol input that ranged from 24 to 160 nmol/m²/d with an average value of 92 nmol/m²/d from July to October in 2007. The differences are 80, 7.8, 2.5, and 1 nmol/m²/d, for the boxes 0–100 m, 100–250 m, 250–850 m, and 850–3500 m, respectively. Assuming steady state condition for the Cd mass in each box, the residence time can be estimated by dividing the total Cd inventory by the Cd flux. The results indicate that
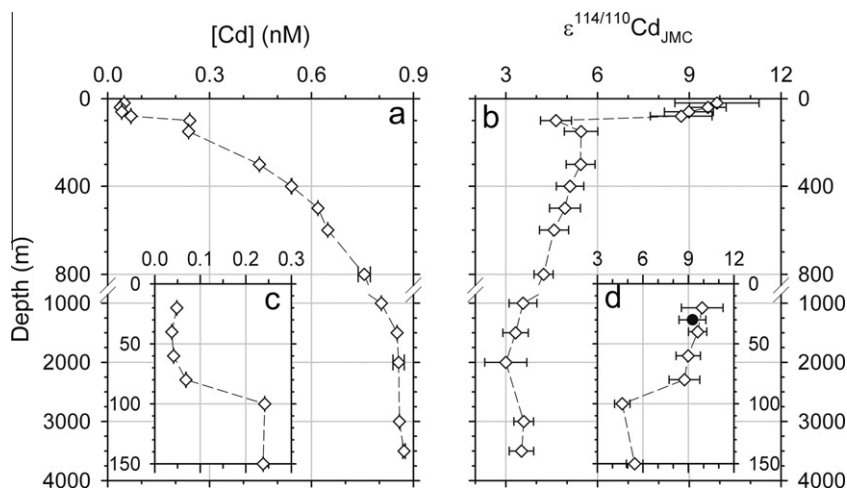

Fig. 3. The vertical profiles of Cd concentration and IC (a) Cd concentration. (b) Cd IC. (c) The concentrations in the top 150 m (d) the Cd IC in the top 150 m. The solid circle symbol stands for the IC in the sinking particles. The error bars for the Cd concentrations and the IC represent standard errors (2SE) of each analysis.
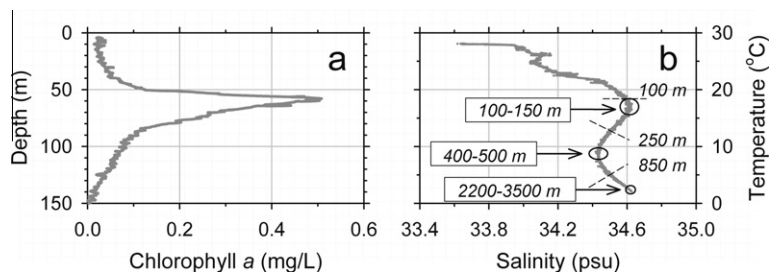
Fig. 4. (a) The vertical profile of chlorophyll *a* concentration in the top 150 m. (b) T–S diagram of the whole water column at the sampling site. The diagram shows that there are three major water masses, the SCS subsurface water at 100–150 m, the SCS intermediate water at 400–500 m, and the SCS deep water at 200–3500 m.
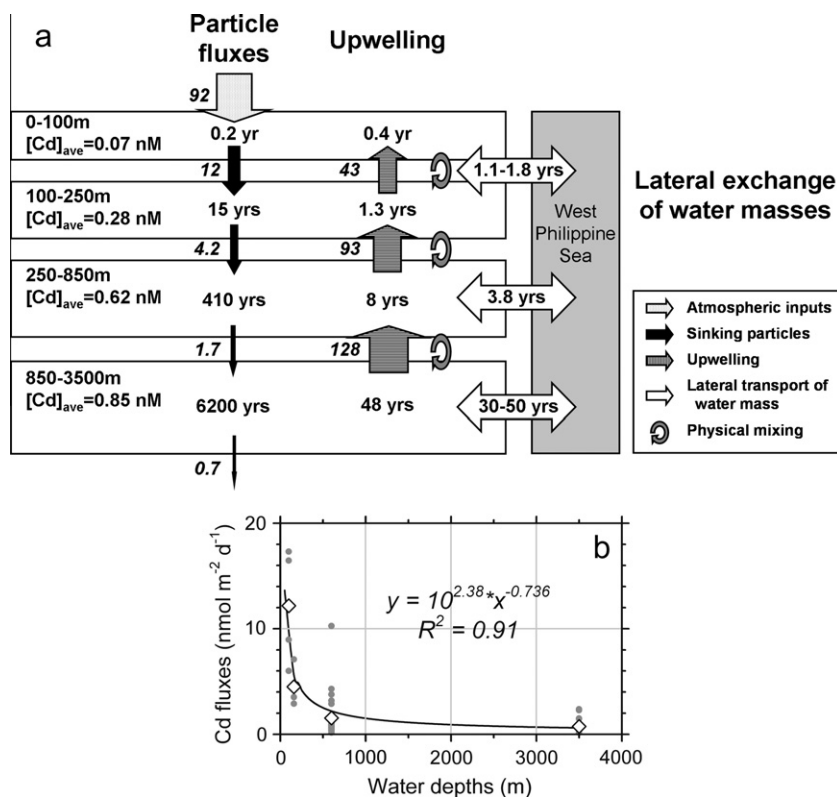

Fig. 5. (a) Box model for Cd cycling in different water columns of the SCS. Annually averaged particle fluxes at 100 and 3500 m are from the studies of sediment traps deployed at these depths (Ho et al., 2009, 2010), and the fluxes at 250 and 850 m are estimated values, for lack of direct observation. It has found that the particle fluxes decrease with depths exponentially, thus we obtained the best regression function for the actual data at 100, 160, 600, and 3500 m depths to estimate the fluxes at 250 and 850 m. Other estimate about concentrations, bottom-up fluxes and turnover times of Cd, see the discussions in 4.1. (b) Regression of Cd fluxes versus water depths.

the residence time in the four boxes from top to the bottom are 0.2, 15, 410, and 6100 years, respectively, simply due to the exponential decrease in the vertical particulate Cd input with depth and the significant increase in the total Cd inventory in the deeper layers. The relatively short Cd residence time in the top two layers indicates that the vertical transport of the sinking particles may be the dominant process in controlling Cd cycling in the layers.

3.2.2. Upwelling and horizontal advection

Vertical upwelling and horizontal advection also control the transport of Cd among different boxes. The bottom-up

transport rates were evaluated and reported by physical and chemical parameters in the studied site, including the use of the mass balance between nutrient supply and the net primary production (Wong et al., 2007), the use of the mass balance between salinity and the water masses (Chen et al., 2001), or the use of physical parameters to estimate water mass upwelling rates (Qu, 2001). The upwelling rates estimated by these studies are similar. Chen et al. (2001) reported that the average upwelling velocity in the SCS is 55 m/year. Wong et al. (2007) found the upward transport velocity to be 41 m/year in the mixing layer, and Qu (2001) reported seasonal upwelling, with 32 m/year in June and

95 m/year in October. Based on these studies, we used 55 m/year as the averaged upwelling velocity in this box model, which results in upward transport with a flux of 128 nmol/m^2/d from the deep box to the thermocline box, 93 nmol/m^2/d from the thermocline box to the subsurface water, and 43 nmol/m^2/d flux from the subsurface box to the surface layer (Fig. 5a). Assuming the steady state of the Cd mass balance in these boxes and the upwelling as the dominant physical vertical mixing process, the residence times are 0.4, 1.3, 8, and 48 years from top to the bottom, respectively.

In terms of the horizontal transport, it is reported that the water mass in the West Philippine Sea (WPS) passes through the Luzon strait and enters the SCS basin (Gong et al., 1992; Qu et al., 2006). Based on the mass balance of water masses and salinity, the vertical transport velocity has been estimated in previous studies. Qu et al. (2006) reported that the residence time of the deep water in the northern SCS basin was roughly around 30 years, similar to the value estimated by Liu et al. (2010), which was 50 years. Liu et al. (2010) also estimated the residence time in the subsurface layer and surface layer, which were 3.8 and 1.5 years, respectively. Based on the comparison of the residence time determined for the vertical transport of sinking particles, upwelling, and horizontal advection, we conclude that the dominant process for controlling Cd cycling in the surface box is particle sinking, and transport of water masses is the primary controlling process in the three deeper boxes.

3.3. The variability in the deep water and the thermocline

The Cd concentration and $\varepsilon^{114/110}$Cd in water deeper than 850 m are 0.8–0.9 nM and +3.5 ± 0.2 (1SD), which are similar to the values in the Northern Pacific Ocean, 0.8–1.0 nM and +3.2 ± 0.5 (Ripperger et al., 2007), and the values in the deep water of the WPS, 0.8–0.9 nM and +3.2 ± 0.7 (unpublished data). The similarity between SCS and the WPS is expected because the SCS deep water originates from the deep water of the WPS (Gong et al., 1992; Qu et al., 2006). Thus, the residence time of Cd would be similar to the residence time of the deep water in the SCS, which is approximately 30–50 years (Qu et al., 2006; Liu et al., 2010). Compared to the input of water transport, the contribution of sinking particles to the dissolved Cd is insignificantly in the deep water of the SCS (Fig. 5a). The averaged residence time estimated via the decomposition of sinking particles was about six thousand years in the deep water column, considerably longer than the residence time of the deep water.

The thermocline and subsurface water, ranging from 850 to 100 m, primarily originates from the horizontal advection of WPS seawater, with a residence time of less than 4 years (Liu et al., 2010). The residence time is also much shorter than the turnover times estimated by the decomposition of sinking particles, which are 410 and 15 years, respectively. In terms of upwelling in the water column, the turnover time in the thermocline and subsurface layers are 8 and 1.3 years, respectively, which are comparable to or slightly longer than the turnover time by horizontal advection. Thus, the Cd isotopic composition reflects the mixing effect between bottom-up upwelling water of the SCS and the thermocline water of the WPS through horizontal advection (Gong et al., 1992; Chao et al., 1996).

The T–S diagram shows that the water column below 100 m is composed of three major water masses (Figs. 4b and 6a), including the bottom water mass deeper than 2200 m, the mid-layer near 400–500 m, and the subsurface layer, ranging from 100 to 150 m. Using these three water masses as end members, the relative mixing ratio at different depths may be estimated by the following equations:

$$\sigma_{\theta,mixed} = V_1\% \cdot \sigma_{\theta,1} + V_2\% \cdot \sigma_{\theta,2}$$
$$V_1\% + V_2\% = 100\%$$

where $\sigma_{\theta,mixed}$ represents the density of water at different depths, $\sigma_{\theta,1}$ and $\sigma_{\theta,2}$ represent the densities of water masses 1 and 2, respectively, and $V_1\%$ and $V_2\%$ represent the rela-
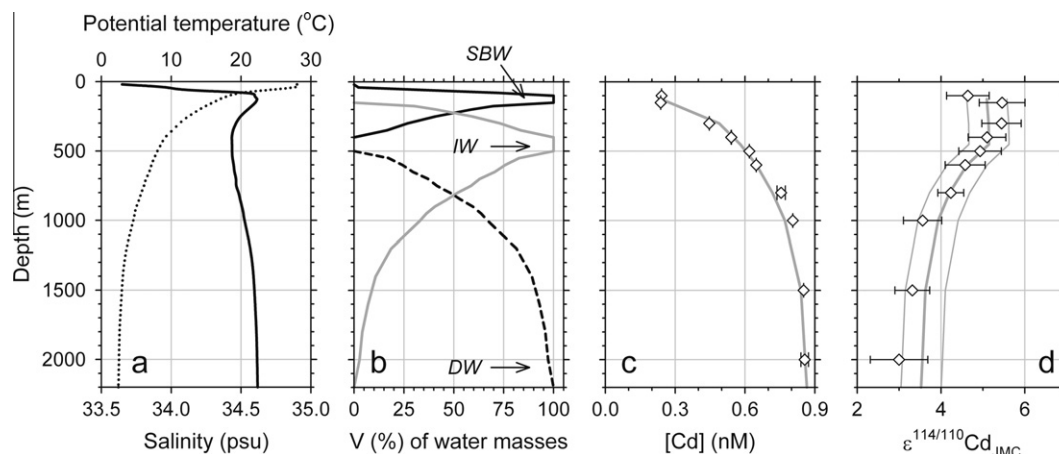

Fig. 6. (a) The vertical profiles of potential temperature (dotted line) and salinity (black line) in the SCS water column. (b) Relative volumetric contribution of the subsurface water (black line), the intermediate water (gray line), and the deep water (dotted line) in the SCS water column. (c) Calculated Cd concentration data (gray line) in a mixing-model and actual Cd concentration data (open diamonds). (d) Calculated Cd isotope data with 95% confidence level (gray line) in a mixing-model and actual Cd isotope data (open diamonds).

tive volumetric ratio of the individual water masses 1 and 2, respectively. The calculated results are shown in Fig. 6b.

Assuming that water mixing is the primary process that determines the Cd concentration and $\varepsilon^{114/110}$Cd in the thermocline and subsurface layers, a simple physical mixing model may be used to calculate theoretical Cd concentration and isotopic composition by using information regarding the relative ratios of the water masses:

$$[Cd]_{Mixed} = V_1\% \cdot [Cd]_1 + V_2\% \cdot [Cd]_2$$

$$\varepsilon^{114/110}Cd_{Mixed}$$
$$= \frac{V_1\% \cdot [Cd]_1 \cdot \varepsilon^{114/110}Cd_1 + V_2\% \cdot [Cd]_2 \cdot \varepsilon^{114/110}Cd_2}{V_1\% \cdot [Cd]_1 + V_2\% \cdot [Cd]_2}$$

where $[Cd]_1$ and $[Cd]_2$ represent the end member Cd concentration for water masses 1 and 2, respectively, $\varepsilon^{114/110}Cd_1$ and $\varepsilon^{114/110}Cd_2$ represent the isotopic composition in water masses 1 and 2, respectively, and $V_1\%$ and $V_2\%$ represent the relative volumetric percentage of water masses 1 and 2 as estimated by the density. The consistent results between the theoretical calculation and the field measured data (Fig. 6c and d) demonstrate that physical mixing generated from vertical upwelling and horizontal advection is the primary process controlling the Cd concentration and isotopic composition in the thermocline of the water column.

3.4. The isotopic composition in the surface water

Ripperger et al. (2007) observed that the Cd isotopic compositions in oceanic deep waters are all similar, at approximately $+3 \pm 0.5$ ε, but the compositions in the surface water could be extremely heavy, ranging from $+10$ to $+38$ ε. They argued that the elevated isotopic compositions in the surface water were most likely attributed to biological fractionation effect, where phytoplankton take up relatively light Cd isotopes and result in relatively heavy isotopes in seawater. The biogenic particles with relatively light Cd isotopic composition are thus brought to the deep oceans, and are regenerated in the deep water to produce the $\varepsilon^{114/110}$Cd of $+3$. By assuming that phytoplankton uptake is the major fractionation mechanism and that the Cd input of subsurface waters is the primary Cd source in oceanic surface waters, the authors proposed that oceanic vertical distribution of Cd isotopic composition generally follows the Rayleigh fractionation model in closed system with fractionation factors (α) ranging from 1.0002 to 1.0006.

The Rayleigh fractionation model proposed by Ripperger et al. (2007) is based on two assumptions: the major Cd source in the surface water originates from the water below the surface layer, and phytoplankton preferentially takes up relatively light Cd in the water. Although our data exhibit a similar concentration–isotopic composition relationship as the data shown in the studies of Ripperger et al. (2007) and Xue et al. (2011), the results of our studies in the SCS are not consistent with the two assumptions. The Cd in the top 80 m zone of the SCS with the lowest concentrations (40–70 pM) also exhibited the highest $\varepsilon^{114/110}$Cd in the water column, ranging from $+9$ to $+10$. At the bottom
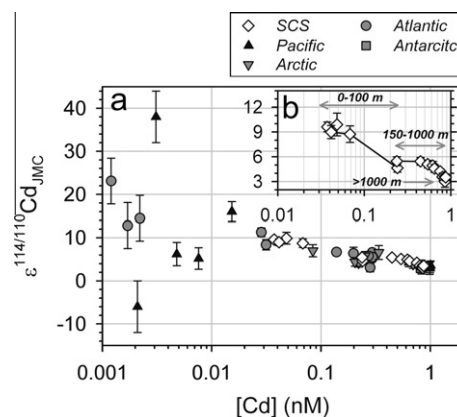

Fig. 7. (a) Variations of both concentration and IC of Cd in the SCS and that of world oceans. The open diamonds denote the data for the SCS, and the closed triangles, closed and gray circles, and gray squares denote the data for the Pacific, Arctic, Atlantic, and Antarctic oceans published in Ripperger et al. (2007) and Xue et al. (2011), respectively. (b) Data for the SCS alone.

of the bioactive zone, near 100 m, the $\varepsilon^{114/110}$Cd decreased to $+4.6 \pm 0.5$, and the concentrations increased to 240 pM (Fig. 7b). The relationship of the concentrations and the Cd isotopic composition seems to follow the Rayleigh fractionation model in a closed system proposed by Ripperger et al. (2007). However, in contrast to the open ocean, anthropogenic aerosols are known to be the major Cd source in the surface water. The Cd fluxes from aeolian deposition are comparable to the fluxes of sinking particles in the mixed layer, indicating that removal rates through biological uptake and particle sinking was relatively high during the high input seasons (Ho et al., 2010). Thus Cd in the sinking particles is largely attributed to the input of anthropogenic aerosols (Ho et al., 2009, 2010) but not from the sub-surface water. The Cd isotopic composition in aerosols samples over the oceanic region can significantly influence the Cd isotopic composition of the surface water in the SCS. Further investigation to determine the Cd isotopic composition in aerosol samples is needed.

Furthermore, the $\varepsilon^{114/110}$Cd of the sinking particles collected at 30 m on October 2006 was $+9.3 \pm 0.9$, which is identical within uncertainty to the $\varepsilon^{114/110}$Cd of dissolved Cd in the ambient seawater, $+9.9 \pm 1.4$ at 20 m and $+9.6 \pm 0.6$ at 40 m. The comparable $\varepsilon^{114/110}$Cd between the sinking particles and the seawater in the surface water indicate that the particle fluxes do not preferentially transport relatively light Cd from the surface water to the deep water.

Based on our previous study, the Cd in the sinking particles in the study site was predominantly intracellular. The Cd/P ratios in the sinking particles, ranging from 0.07 to 0.17 mmol/mol, were comparable to or slightly lower than known intracellular Cd quota in marine phytoplankton, which are 0.42 ± 0.20 mmol/mol (Ho, 2006). In contrast to Cd, many other biologically essential metals were 1–2 orders of magnitudes higher than their intracellular quotas (Ho et al., 2010). In addition, abiotic Cd such as lithogenic Cd in the sinking particles was negligible. The Cd/Al ratio

Table 2
The Al and P normalized elemental ratios in the sinking particle sample.

Elemental ratios (mmol/mol)[a]	Fe	Mn	Zn	Co	Cd	Pb
Relative to Al	752	14	47	0.88	0.28	35
(Crustal ratio)[b]	(252)	(5.7)	(0.54)	(0.18)	(0.0006)	(0.043)
Relative to P	177	3.4	11	0.21	0.07	8
(Intercellular ratio)[c]	(3.6–7.4)	(0.3–1.6)	(0.8–3.0)	(0.10–0.19)	(0.07–0.54)	–

[a] Calculated from the data published in Ho et al. (2010).
[b] Calvert et al. (1993).
[c] Ho (2006).

in the sinking particle sample analyzed in this study, 0.28 mmol/mol, was 2 orders of magnitude higher than the Cd ratio in lithogenic particles, 0.0006 mmol/mol (Table 2), indicating that the contribution of lithogenic Cd in the sinking particles is less than 0.2% of total Cd in the sinking particles.

The vertical concentration gradients of organic carbon and phosphorus fluxes in the euphotic zone of the study site provide us the other approach to further quantitatively estimate the contribution of biogenic Cd in the sinking particle (Ho et al., 2010). The vertical variations of Cd fluxes in sinking particles were linearly proportional to the variations of organic C and P fluxes (Ho et al., 2010). Based on the flux difference of Cd or organic matter between 30 and 160 m, about 90% of particulate Cd and organic matter at 30 m was remineralized through microbial degradation once the particles reached 160 m (Ho et al., 2010). The Cd to P ratios in the sinking particles at 160 m, ranging from 0.06 to 0.12 mmol/mol, still remained close to or slightly lower than known intracellular quotas in phytoplankton (Ho et al., 2010). Thus, the Cd in the sinking particles at 160 m was still dominantly biogenic. Overall, more than 99% of Cd in the sinking particles collected at 30 m was biogenic, and the contribution of other abiotic particles (e.g., lithogenic and anthropogenic particles) was negligible.

The adsorption of Cd on the sinking particles might influence the isotopic composition in the sinking particles. However, no Cd adsorption behavior was observed in the surface water. Theoretically, Cd adsorption on sinking particles would increase Cd to P ratios in the particles. Although the Cd concentrations increased from 40 to 240 pM between 30 and 150 m, the Cd to P ratios in the sinking particles still remained consistent from 30 to 150 m (Ho et al., 2010). The Cd to P ratios in various sizes of phytoplankton and plankton, which possessed different area to volume ratios, were statistically identical (Ho et al., 2009). Moreover, the Cd concentrations in the top 60 m mixed layer were fairly consistent (Wen et al., 2006), indicating that no significant net dissolution effect occurred out of sinking particles from the surface water to 30 m.

Because the Cd in the sinking particles was predominantly intracellular, the comparable isotopic composition between the sinking particles and the seawater in the surface water indicates that there was no significant net biological fractionation in the surface water (Fig. 3d). Overall biological activities in the surface water do not seem to preferentially take up relatively light Cd from the surface water.

Ripperger et al. (2007) proposed that the uptake of lighter Cd by phytoplankton may be attributed to Zn depletion in seawater. Analyzing the Cd isotopic composition in the surface water of the Weddell Gyre and the Antarctic Circumpolar Current, Abouchami et al. (2011) observed that phytoplankton had different Cd isotopic fractionation effects in the two oceanic regions, with fractionation factors to be 1.0002 and 1.0004, respectively. The authors proposed that the fractionation may be attributed to the phytoplankton community structure or the availability of the associated metals like Zn or Mn. It should be noted that extracellular membrane transporters can play critical roles on controlling the isotopic composition of trace metals (John et al., 2007), and the property of the transporters can be influenced by various environmental factors, such as the bioavailability of Mn, Zn, and Fe (Sunda and Huntsman, 2000; Lane et al., 2009). It is possible that the bioavailability of these associated metals can influence the fractionation effect of phytoplankton on Cd.

In the SCS, our previous studies have shown that trace metal input to the surface water is high due to elevated anthropogenic aerosol deposition in the oceanic region. Phytoplankton adsorb a significant amount of trace metals originating from anthropogenic aerosols (Ho et al., 2007, 2009, 2010). The Zn and Mn extracellularly adsorbed by phytoplankton were approximately one order of magnitude higher than their averaged intracellular quotas (Ho et al., 2003). Thus, Zn and Mn are unlikely to be limiting factors for phytoplankton growth in the surface water. The insignificant difference in the Cd isotopic composition between the surface water and the biogenic particles suggests that phytoplankton in the water did not significantly fractionate Cd isotopic composition under sufficient trace metal availability. Further laboratory culture experiments are needed to demonstrate the biological fractionation effect on Cd isotopes by using specific phytoplankton under depleted or replete conditions of the associated trace metals.

4. CONCLUSIONS

The Cd isotopic composition and concentrations observed in the water column of the SCS exhibit similar trends as those reported in a previous study (Ripperger et al., 2007), showing a nearly linear relationship between the isotopic composition and log scale concentrations. However, the variations of the isotopic composition and concentrations of Cd in the thermocline and the deep water were relatively conservative, closely following the relative

volumetric contribution of water masses in different layers. In addition, the $\varepsilon^{114/110}$Cd of the seawater and sinking particles in the surface water ranged from +9 to +10, without significant difference. Both observations indicate that net biological fractionation of the $\varepsilon^{114/110}$Cd is not significant in the surface water, and the Rayleigh distillization model may not apply to explain the vertical variability of the Cd isotopic composition in the ocean at least in the SCS. Because our previous study demonstrated that the surface water of the SCS is trace metal replete, the heavy Cd isotopic composition observed in the seawater and sinking particles in the surface water may be attributed to the input of anthropogenic aerosols in the oceanic region.

ACKNOWLEDGMENTS

APPENDIX A. SUPPLEMENTARY DATA

Supplementary data associated with this article can be found, in the online version, at http://dx.doi.org/10.1016/j.gca.2012.09.022.

REFERENCES

Abouchami W., Galer S. J. G., de Baar H. J. W., Alderkamp A. C., Middag R. and Laan P. (2011) Modulation of the Southern Ocean cadmium isotope signature by ocean circulation and primary productivity. *Earth Planet. Sci. Lett.* **305**, 83–91.

Abouchami W., Galer S. J. G., Horner T. J., Rehkämper M., Wombacher F., Xue Z., Lambelet M., Gault-Ringold M., Stirling C. H., Schönbächler M., Shiel A. E., Weis D. and Holdship P. F. (2012) A common reference material for cadmium isotope studies – NIST SRM 3108. *Geostand. Geoanal. Res.* http://dx.doi.org/10.1111/j.1751-908X.2012.00175.x.

Boyle E. A., Sclater F. and Edmond J. M. (1976) Marine geochemistry of cadmium. *Nature* **263**, 42–44.

Boyle E. A. (1988) Cadmium: chemical tracer of deep-water paleoceanography. *Paleoceanography* **3**, 471–490.

Bruland K. W. (1980) Oceanographic distributions of cadmium, zinc, nickel, and copper in the North Pacific. *Earth Planet. Sci. Lett.* **47**, 176–198.

Calvert S. E., Pedersen T. F. and Thunell R. C. (1993) Geochemistry of the surface sediments of the Sulu and South China Seas. *Mar. Geol.* **114**, 207–231.

Chao S. Y., Shaw P. T. and Wu S. Y. (1996) Deep water ventilation in the South China Sea. *Deep-Sea Res. Oceanogr.* **43**, 445–466.

Chen C. T. A., Wang S. L., Wang B. J. and Pai S. C. (2001) Nutrient budgets for the South China Sea basin. *Mar. Chem.* **75**, 281–300.

Elderfield H. and Rickaby R. E. M. (2000) Oceanic Cd/P ratio and nutrient utilization in the glacial Southern Ocean. *Nature* **405**, 305–310.

Gault-Ringold M. and Stirling C. H. (2012) Anomalous isotopic shifts associated with organic resin residues during cadmium isotopic analysis by double spike MC-ICPMS. *J. Anal. At. Spectrom.* **27**, 449–459.

Gong G. C., Liu K. K., Liu C. T. and Pai S. C. (1992) The chemical hydrography of the South China Sea West of Luzon and a comparison with the West Philippine Sea. *TAO* **3**, 587–602.

Ho T. Y., Quigg A., Finkel Z. V., Milligan A. J., Wyman K., Falkowski P. G. and Morel F. M. M. (2003) The elemental composition of some marine phytoplankton. *J. Phycol.* **39**, 1145–1159.

Ho T. Y. (2006) The trace metal composition of marine microalgae in cultures and natural assemblages. In *Algal Cultures: Analogues of Blooms and Applications* (ed. D. V. Subba Rao). Science Pub. Inc., New Hampshire, USA, pp. 271–299.

Ho T. Y., Wen L. S., You C. F. and Lee D. C. (2007) The trace-metal composition of size-fractionated plankton in the South China Sea: biotic versus abiotic sources. *Limnol. Oceanogr.* **52**, 1776–1788.

Ho T. Y., You C. F., Chou W. C., Pai S. C., Wen L. S. and Sheu D. D. (2009) Cadmium and phosphorus cycling in the water column of the South China Sea: the roles of biotic and abiotic particles. *Mar. Chem.* **115**, 125–133.

Ho T. Y., Chou W. C., Wei C. L., Lin F. J., Wong G. T. F. and Lin H. L. (2010) Trace metal cycling in the surface water of the South China Sea: vertical fluxes, composition, and sources. *Limnol. Oceanogr.* **55**, 1807–1820.

John S. G., Geis R. W., Saito M. A. and Boyle E. A. (2007) Zinc isotope fractionation during high-affinity and low-affinity zinc transport by the marine diatom. *Thalassiosira oceanica. Limnol. Oceanogr.* **52**(6), 2710–2714.

Lacan F., Francois R., Ji Y. C. and Sherrell R. M. (2006) Cadmium isotopic composition in the ocean. *Geochim. Cosmochim. Acta* **70**, 5104–5118.

Lane E. S., Semeniuk D. M., Strzepek R. F., Cullen J. T. and Maldonado M. T. (2009) Effects of iron limitation on intracellular cadmium of cultured phytoplankton: implications for surface dissolved cadmium to phosphate ratios. *Mar. Chem.* **115**, 155–162.

Lin I. I., Chen J. P., Wong G. T. F., Huang C. W. and Lien C. C. (2007) Aerosol input to the South China Sea: results from the MODerate resolution Imaging Spectro-radiometer, the quick scatterometer, and the measurements of pollution in the troposphere sensor. *Deep-Sea Res. Oceanogr.* **54**, 1589–1601.

Liu K. K., Tseng C. M., Wu C. R. and Lin I. I. (2010) The South China Sea. In *Carbon and Nutrient Fluxes in Continental Margins: A Global Synthesis* (eds. K. K. Liu, L. Atkinson, R. Quiñones and L. Talaue-McManus), pp. 464–482. IGBP Book Series. Springer, Berlin.

Pai S. C., Fang T. H., Chen A. C. T. and Jeng K. L. (1990) A low contamination Chelex-100 technique for shipboard preconcentration of heavy metals in seawater. *Mar. Chem.* **29**, 295–306.

Qu T. D. (2001) Role of ocean dynamics in determining the mean seasonal cycle of the South China Sea surface temperature. *J. Geophys. Res.* **106**. http://dx.doi.org/10.1029/2000JC000479.

Qu T. D., Girton J. B. and Whitehead J. A. (2006) Deepwater overflow through Luzon Strait. *J. Geophys. Res.* **111**. http://dx.doi.org/10.1029/2005JC003139.

Qu T. D., Mitsudera H. and Yamagata T. (2000) Intrusion of the North Pacific waters into the South China Sea. *J. Geophys. Res.* **105**. http://dx.doi.org/10.1029/1999JC900323.

Ripperger S. and Rehkamper M. (2007) Precise determination of cadmium isotope fractionation in seawater by double spike MC-ICPMS. *Geochim. Cosmochim. Acta* **71**, 631–642.

Ripperger S., Rehkamper M., Porcelli D. and Halliday A. N. (2007) Cadmium isotope fractionation in seawater – a signature of biological activity. *Earth Planet. Sci. Lett.* **261**, 670–684.

Shiel A. E., Barlin J., Orians K. J. and Weis D. (2009) Matrix effects on the multi-collector inductively coupled plasma mass spectrometric analysis of high-precision cadmium and zinc isotope ratios. *Anal. Chim. Acta* **633**, 29–37.

Sunda W. G. and Huntsman S. A. (2000) Effect of Zn, Mn, and Fe on Cd accumulation in phytoplankton: implications for oceanic Cd cycling. *Limnol. Oceanogr.* **45**(7), 1501–1516.

Wen L. S., Jiann K. T. and Santschi P. H. (2006) Physicochemical speciation of bioactive trace metals (Cd, Cu, Fe, Ni) in the oligotrophic South China Sea. *Mar. Chem.* **101**, 104–129.

Wong G. T. F., Tseng C. M., Wen L. S. and Chung S. W. (2007) Nutrient dynamics and N-anomaly at the SEATS station. *Deep-Sea Res. Oceanogr.* **54**, 1528–1545.

Xue Z., Rehkämper M., Schönbächler M., Statham P. J. and Coles B. J. (2011) A new methodology for precise cadmium isotope analyses of seawater. *Anal. Bioanal. Chem.*. http://dx.doi.org/10.1007/s00216-011-5487-0.

Associate editor: Derek Vance